2

Application of Thermography in Materials Science and Engineering

Alin Constantin Murariu, Aurel - Valentin Bîrdeanu, Radu Cojocaru, Voicu Ionel Safta, Dorin Dehelean, Lia Boțilă and Cristian Ciucă
National R&D Institute of Welding and Materials Testing – ISIM Timişoara
Romania

1. Introduction

The chapter presents the main applications of IR thermography in material science and engineering with focus on modern methods for examination of materials and applications in new processing technologies development and to the improvement of existing processing technologies by implementing process control. Beside a synthesis of the applications presented in the existing literature, applications of IR thermography developed by the chapter's authors are presented. The following subchapters will present various applications of IR thermography in materials science and engineering.

Infrared thermography is a one of the modern imaging methods which allows the temperature assessment of an object by contactless testing, with a wide range of possible applications both in materials science and in engineering. Most applications are related to non-destructive testing and monitoring of equipments, components or different technological processes.

In material science, destructive test methods provide information regarding the initial structure and material's strength characteristics or an estimation of these at different operating durations, in order to assess the service life of the components in safety critical conditions. For the modern new product's development strategies, the selection of the engineering material process has to take into account the material's in-time-stability characteristics. Due to this trend, new examination techniques, which are based on material fracture concept and theories, have been developed for studying and complete characterization of the new materials types.

2. Application of thermography in materials science

The relationship between temperature and material deformation was recognized in 1853 by Kelvin and then developed by Biot, Rocca, and Bever in the 1950s (Yang, B. et al., 2003). In 1956, Belgen developed IR radiometric techniques for detecting temperature changes and in the 1960s, Dillon and Kratochvil developed the thermoplastic theory that directly relates the temperature with the material internal stress-strain state, which, in turn, controls the mechanical and fatigue behaviour (Yang, B. et al., 2003). Active thermography allows the detection and the characterization of exfoliation between layers (Rajic, 2004) in different

stages of testing and the passive one allows the localization of crack initiation. In case of composite materials, especially for "sandwich" structure type, active and passive infrared thermography (Balageas, et Al., 2006) became a current technique to monitor the mechanical testing.

Elaboration of the new materials or the properties improvement of the existing ones represents one of the major priority directions in the research field of thermoplastics and composite materials. Before launching of the new product or the material on the market, they must be tested in order to assess their in-service usage ability for the specific exploitation conditions. Recent research (Avdelidis et al., 2010; Bremond, 2010; Choi et al., 2008; Galietti & Palumbo 2010; Huebner et al., 2010; Kruczek, 2008; Murariu et al., 2010; Pieczyska et al. 2008; Sahli et al. 2010; Thiemann, 2010) has shown the potential of thermography in the monitoring of the mechanical damage but, at the same time, more detailed investigations and analyses are needed in order to develop a more practical thermography method for characterizing the materials' proprieties. In the following section some applications of thermography in materials science are presented.

2.1 Application of active thermography for quality assessment of PEHD pipes

The use of thermoplastic materials in the pipes networks was developed due to their advantages while compared to the use of metallic materials: greater corrosive resistance, low weight, good mechanical strength, high resistance to the aggressive fluids, low hydraulic losses, flexibility etc. A special utilization is given to the high density polyethylene (HDPE) for assemble of pipes networks for gases or water distribution.

Using the active thermography, a method for quality assessment of HDPE pipes was developed and, in order to reveal the new method's sensitivity, an experimental program was designed using pipe specimens with longitudinal simulated imperfections. The imperfections were performed using Laser Simulated Imperfection - LSI method (Murariu & Bîrdeanu, 2007), and activation was done with water at 80°C. For simulating the imperfections in the base material a Nd:YAG laser Trumpf HL 124P LCU (Trumpf GmbH, Ditzingen, Germany) with a fibreglass connected cutting head was used (figure 1).

Fig. 1. LSI experimental setup

For simulating the imperfections, the laser process parameters were specific to pulsed laser beam cutting, i.e. short width rectangular pulses, relative high pulse peak power and high pulse repetition rate (55Hz) in respect to the travelling speed (3.73mm/s). As processing gas, Ar99% at 6bar pressure was used. Experiments were performed to establish the process parameter adjustment space according to the desired penetration depths for the specimens. The data showed an appropriate linearity for penetration depending on the pulse peak power, so a programmed experiment was performed to establish the equation that correlates the penetration depth to the peak power pulse.

The data was graphically fitted (figure 2) and the corresponding equation describing the penetration depth variation as a function to the pulse peak power for the targeted domain was established. Using the mathematical equation it was possible to calculate the pulse power peak necessary to simulate the required imperfections in the material. Furthermore, the calculated parameters were verified by doing a set of experiments and measuring the penetration depths and it was determined that the measured data corresponded to the calculated one in respect to the experimental errors.

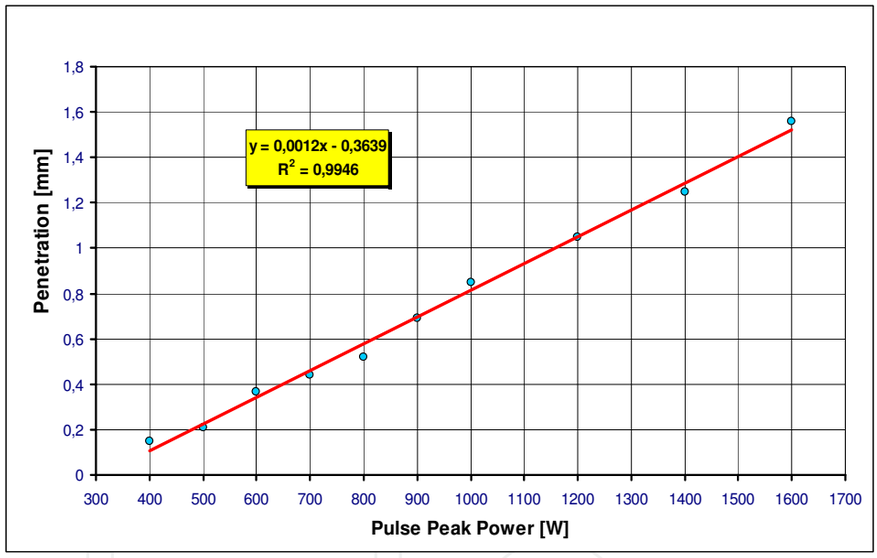

Fig. 2. LSI calibration - fitted experimental data

In order to estimate the sensitivity of the method, an experimental program was performed using PE80, DN 32, SDR11, GAS pipes and the longitudinal notch with depths between 0.15 mm and 1.5 mm have been created using LSI method. Thermographic examination results are shown in Figure 3. The thermographic images were analyzed and the imperfections were revealed. The minimum notch depth which could be detected was h=0.15mm for a pipe with wall thickness e=3.0mm (imperfection has a relative size of A=5% of the component wall thickness) but one could consider that the use of an automated computer analysis of the thermographic images, can improve the limit of the detection.

After the calibration and the evaluation of the method's sensitivity, experimental measurements were performed on pipes with real flaws obtain by hydrostatic inner pressure at constant temperature after different testing durations. The results are shown in Figure 4.

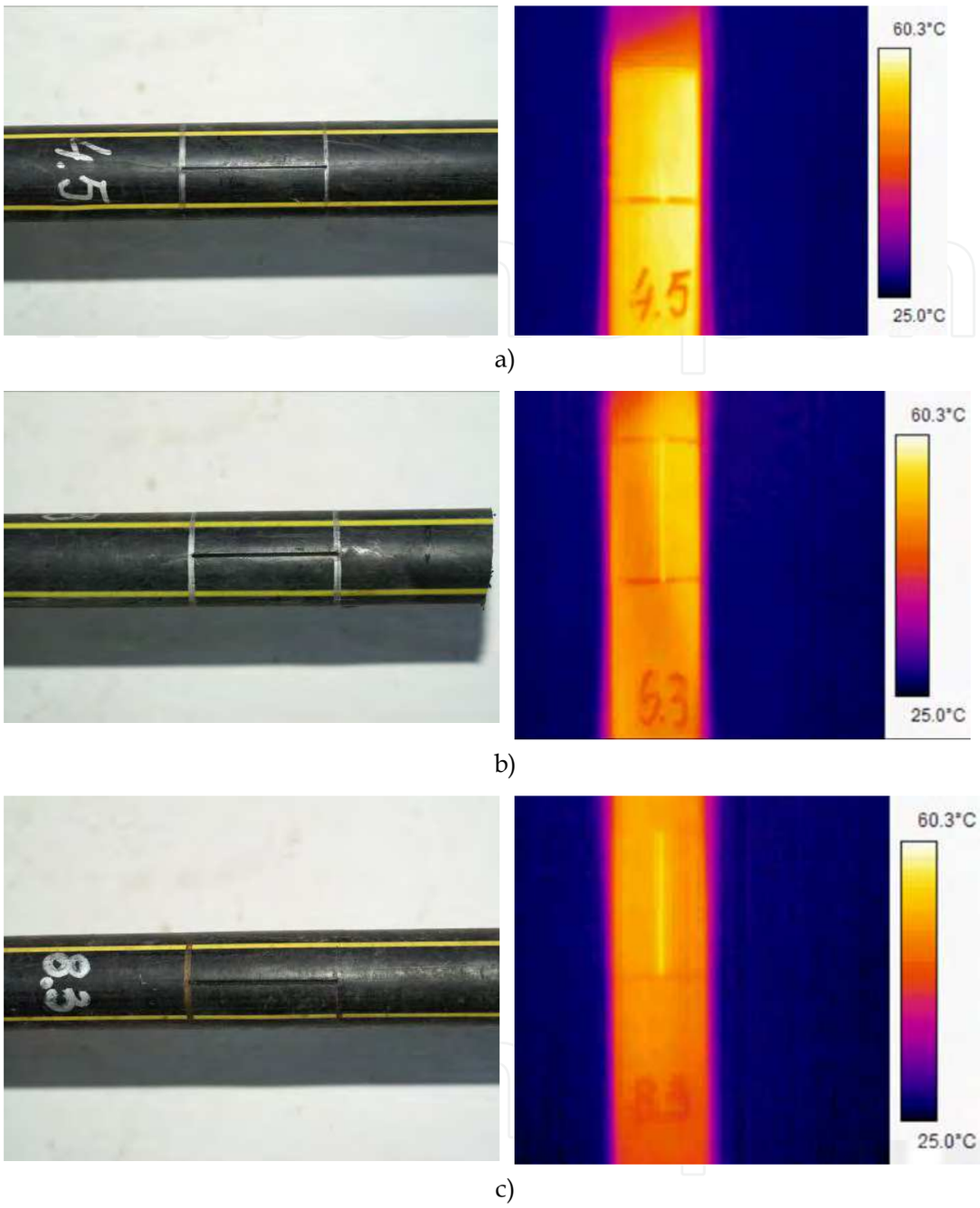

a) relative notch depth A=5% of the pipe wall thickness b) relative notch depth A=10% of the pipe wall thickness c) relative notch depth A=40% of the pipe wall thickness

Fig. 3. PE 80 pipes with LSI simulated imperfections examined by thermography

The experiment did show that by using thermography method and transient temperature regime obtained by thermal activation with warm water, filiform defects of thermoplastic pipes can be detected. This rather fast and accurate method can also detect defects which are sometimes more difficult to identify using other NDT methods, e.g. ultrasound, X-Ray.

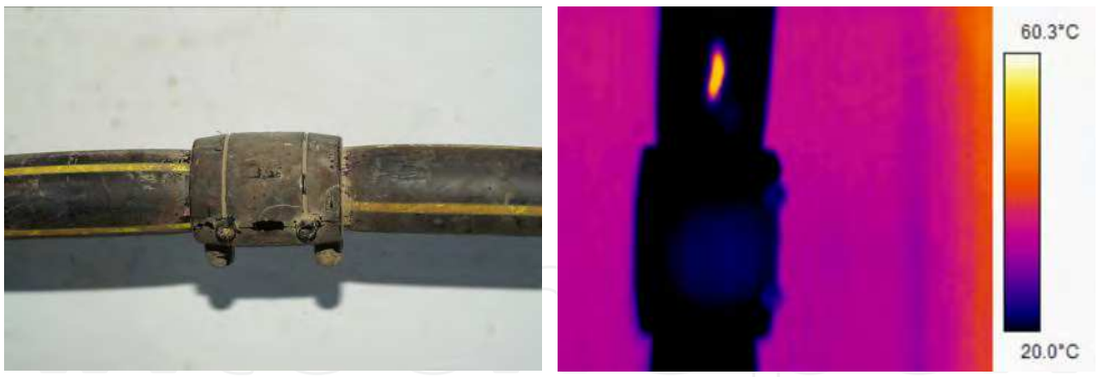

a)

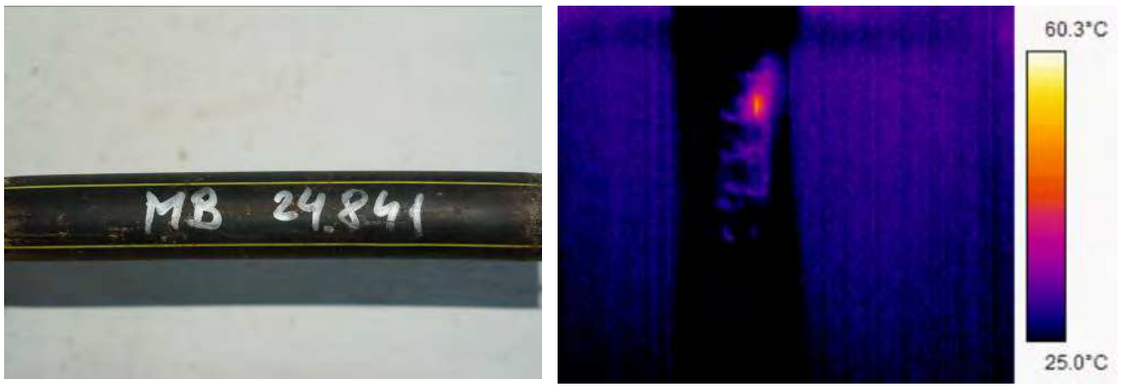

b)

Fig. 4. PE 80 pipes with flaws obtained on hydrostatic inner pressure test at a constant temperature (80°C and 10 bar); a) sleeve welded joints with flaws in the MB, b) PE 80 pipe cracked after 24841 hours of testing

2.2 Application of TT - IRT hybrid technique on thermoplastic materials

To assess the deformation and fracture behaviour of polymers, hybrid test techniques that combine the classical mechanical tests with the non-destructive examinations (i.e. acoustic emission, thermography, laser extensometry) can be applied. By applying these hybrid techniques, quantitative properties – morphology correlations can be made. Most of the materials heat up when they are loaded beyond elastic limit. Starting from this observation, for studying the polyethylene's behaviour in the presence of simulated plane imperfections, thermography method was used to display the heat emission of the specimen. A chapter presents the application of Tensile Test monitored by Infrared Thermography hybrid technique TT-IRT (Murariu, 2007) in order to put in evidence the noxiousness of geometric imperfections that can appear on pipes networks. Thermography method allows analyzing the polyethylene fracture behaviour due to simulated imperfections. The temperature changes in thermographic images of specimens during the tensile test allow studying of local deformation process of thermoplastic polymer.

The following is an example of the TT-IRT hybrid technique use for fracture behaviour study of PE 80 type thermoplastic material. The method may be also applied to other

thermoplastics or advanced materials for stress raiser sensibility evaluation of materials or products in the elaboration/fabrication phase and also after an in-exploitation duration. The experimental program used samples extracted from PE 80 SRD 11 GAS ϕ160×15.5 mm polyethylene pipes. Strip samples with width b=20.0 mm and thickness a=15.5 mm were cut from sample pipes with length L=200 mm. Simulated imperfections were realized by mechanical processes (milling) and consisted in transversal cuttings with angle of the flanks of 45° and with top radius of 0.25 mm (figure 5). Five sets of ten samples with notch depth h=1.0, 1.5, 2.0, 2.5 and 3.0mm were prepared.

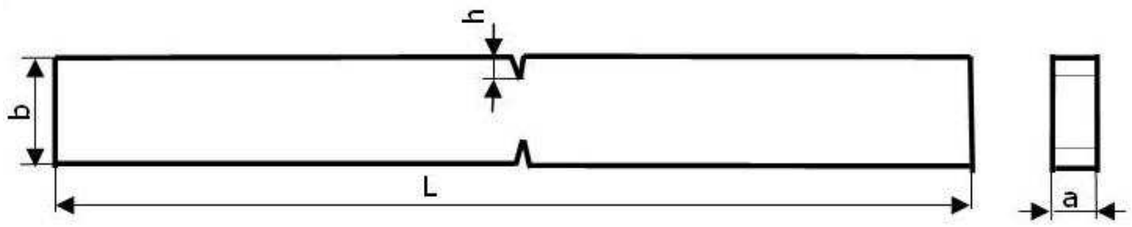

Fig. 5. Blueprint of the samples with bilateral V notch

The experimental setup included a universal mechanical testing machine, an air conditioning room and an infrared thermography camera. The clamping dies speeds of the tensile loading machine were, v=1, 5, 10, 25, 50, 75, 100, 125, 150 and 650mm/min. The test was performed at room temperature (23±2°C). The thermographic camera did record the caloric energy emission during the tensile loading process of the sample and temperatures of the interest zones (stress raisers zone created by the presence of the plane imperfections) were monitored. The method did allow the analyses of the thermal image of the tested samples, which distribution is modified during the testing. The surface temperature values in the imperfection simulated zone were recorded and correlated with the applied stress levels. Thus the method allows studying of the defects' severity and their evolution together with the reaction of the adjacent material due to loading process. The tests proved the tensile strength, the identification of the fracture type and the fracture position, under controlled tests condition: temperature, loading rate. It was determined that the recorded temperatures during the tensile tests are correlated with the local stress condition induced by the loading of the specimen which has geometrical discontinuities. Also it was highlighted that the sample failure is determined by the appearance of "hot" spots in the breaking cross-section. This spots are specific to each type of imperfection and do determine the sample's failure dynamic. Figure 6 shows the possibility of using infrared thermography to failure dynamics analysis of samples with simulated defects.

Next, to prove the way in which the temperature modifications during the testing do influence the failure's character, the aspect of the tested samples' surface failure was analyzed in cases of samples for which the notched area represents 10 and 30% of the transversal cross section of the sample. Figure 7 presents the surface aspect of a sample fracture by axial loading with clamping dies speed of 650mm/min. The sample presents bilateral V notches with h=1mm depth, occupying 10% from the transversal cross section area. Figure 8a, presents the fracture surface of a sample with bilateral V notches with h=3mm depth, affecting 30% of the transversal cross-section area. The tests were similar to the previous ones. One can observe that, depending on the fracture's character, the sample

Frontal view Lateral view Frontal view Lateral view

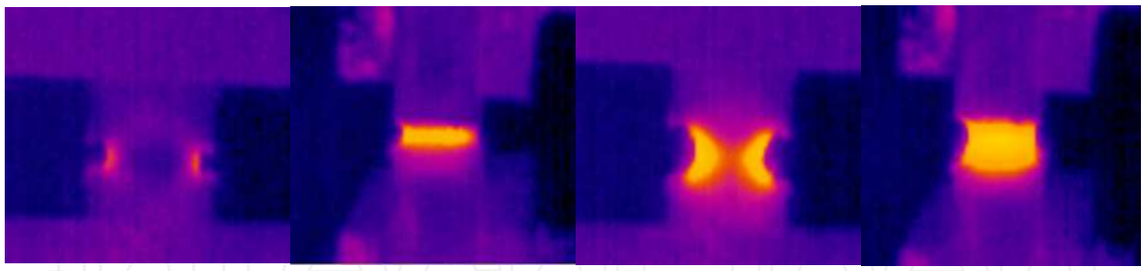

a – The sample heating in the notch and its deformation

b – The heat propagation to the centre of the sample until the thermal fields join

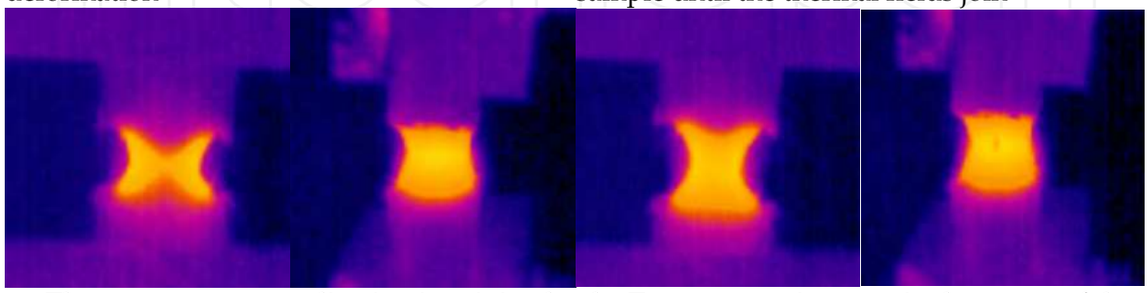

c – The temperature equalization in minimal cross-section of the sample

d – Temperature increase in the centre of the sample in minimal cross section and the leak formation

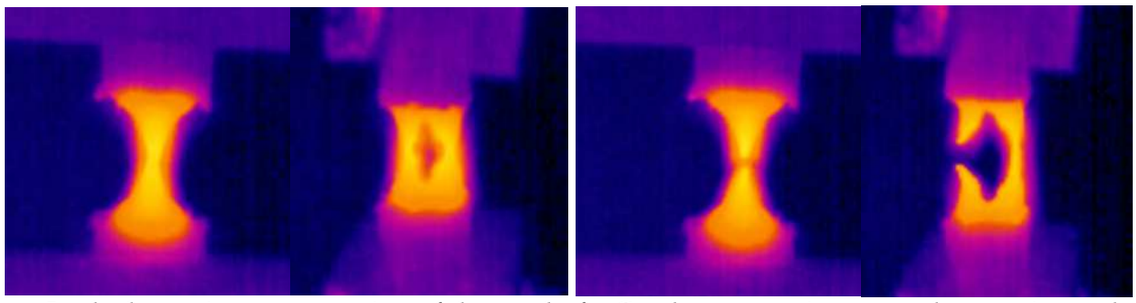

e – Leak elongation, propagation of the crack, initiated from the leak

f – Crack propagation up to the exterior and sample failure

Fig. 6. The fracture dynamic of a sample with V notch

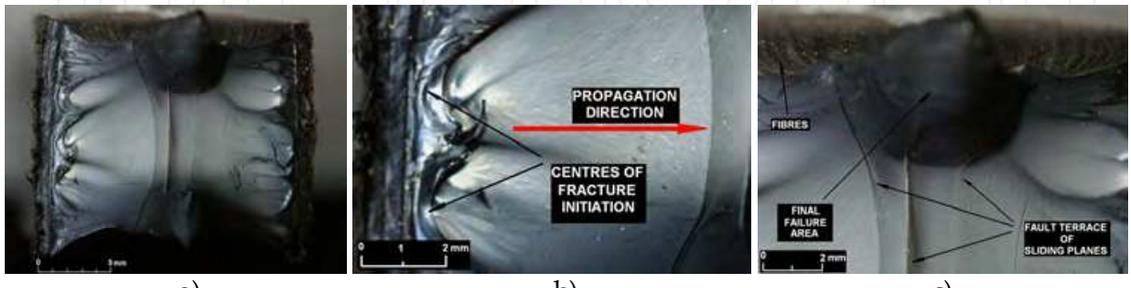

a) b) c)

Fig. 7. The breaking surface of a sample with bilateral V notches with h=1mm depth and v=650 mm/min.; a - failure surface, b - aspect of the fracture initiation zone, c – aspect of the final fracture zone.

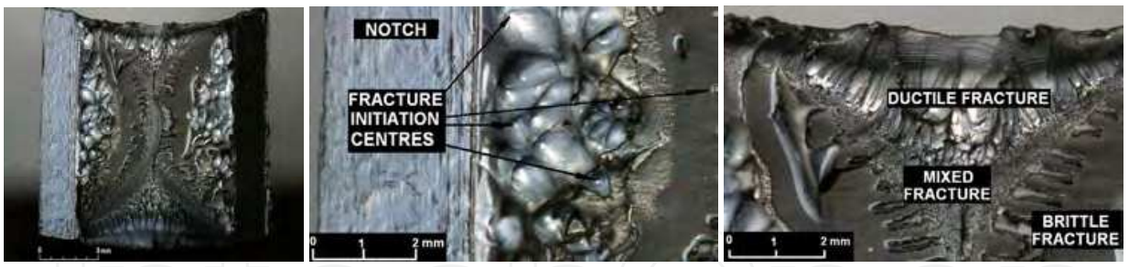

a. b. c.

Fig. 8. The breaking surface of a sample with bilateral V notch with h=3 mm depth and v=650mm/min.; a – The breaking surface, b – The breaking initiation centres, c –The areas with ductile, fragile or mixed breaking

presents bi-axial symmetry. In the transversal fracture surface of the sample multiple fracture initiation centres (figure 8b) are observed with a spherical shape when they are single, or elongated if they are grouped. In the fracture surface both ductile fracture areas, with significant deformations and slipping areas near the breaking initiation centre, and fragile fracture areas without significant deformations (figure 8c) are present.

The modification of the fracture's character is explained by the difference in the sample temperatures in the transversal cross section, during the tensile test. Thus, the sample's temperature is higher in the V notch which is a stress raiser and in the centre of the lateral surfaces, a fact that was confirmed by thermography. The apparition of the fragile failure is explained by the fact that the test was made at high rate (v=650mm/min.) in the conditions of a 30% decrease of the fracture's section. Because the time was insufficient to achieve a uniform temperature in the transversal cross section, the sample fracture took place by different failure mechanisms; the fracture's character was influenced by the local stress distribution and temperature.

While the presented above examples do reveal the practical use of the TT-IRT hybrid technique for studying the fractures behaviour for PE 80 type thermoplastic material, the method may be also applied to other thermoplastics or advanced materials for stress raiser sensibility evaluation of materials/products in the elaboration/fabrication phase and after an in-exploitation duration. Also the results may be useful for studying a fracture behaviour for typical planar imperfection from the butt welded joints of thermoplastic pipes, under different loading conditions, in order to assess the critical imperfection which leads to the joints failure.

3. Application of thermography in engineering

Infrared thermography is a modern imaging method which allows the assessment of the temperature of an object by contactless testing, with multiple possible applications in the field of non-destructive testing and monitoring of equipment, component and technological processes.

3.1 Lack of adhesion defect identification in thermal spraying layer

The section presents an application of active thermography for the process quality evaluation of thermal spraying coated surfaces. The thermal sprayed layers are commonly

used in industrial applications aiming to protect certain severely loaded components. Depending on the specific application, they may be used as thermal barriers for base material's protection, for increasing the wear resistance or corrosion resistance in aggressive environments. A layer deposited by thermal spraying is usually characterized by: adhesion, structure, density and porosity. The adherence is one of the basic characteristics of the deposited layer which insures the strength, the durability and the protection level of the coated components. The evaluation of the thermal sprayed layers using the active thermography method is based on the physical phenomenon according to which any natural object is emitting a thermal radiation consisting of the radiation emitted at rotational and vibrational quantum level transitions, and of the reflected radiation, due to other thermal sources. The visualization technique of the infrared images obtained based on the characteristics of the thermal emission of objects is generically known as the thermo vision or thermography technique.

By thermography one does put in evidence the thermal field on the surface of the tested component. The presence of an imperfection located on the component's surface or in its vicinity acts as a thermal barrier that influences the thermal field's propagation at the surface. As a result, the inhomogeneity of thermal properties of the tested component, or the presence of some imperfections, is revealed as temperature variations of the component's surface. When heating and testing are performed on the same side of the component, the flaw indication appears as a hotter spot (hot flaws). When heating is performed on one side and testing is done on the other side, the flaw indication appears as a colder spot (cold flaws). Thus, the temperatures' distribution on a tested surface can be used to identify and localize the flaws hidden inside the coating material (lack of adherence between the coating layer and the base metal), excessive thickness of the coating and air infiltrations between the components of a sandwich-type structure and for the case with imperfections hidden in the various components' joints.

The following is an example of active thermography used for quality assessment of thermal spray coated surfaces. The proposed activation system (figure 9) is composed of 2 generators and two flashbulb based lamps with the necessary accessories, which ensure the activation energy and its uniform distribution on the tested object. To evaluate the quality of the layers deposited by thermal spraying, using the active thermography method, artificial defects were machined on testing specimens according to an experimental program using

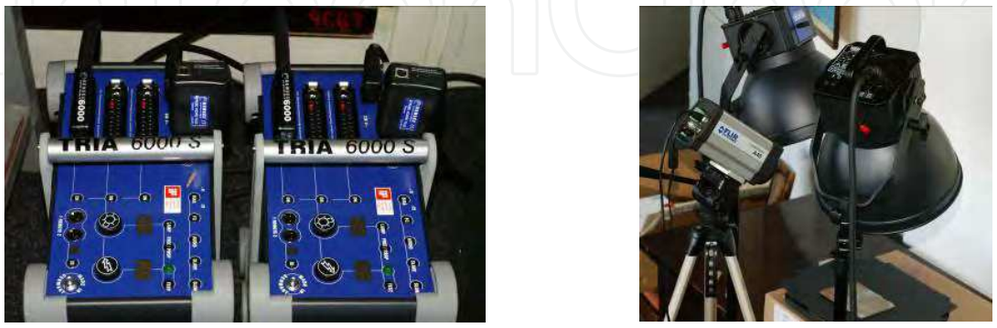

a) b)

a) Generators; b) Flash lamps and thermographic camera

Fig. 9. Activation system – experimental setup

electric-arc thermal spraying process. The base material consisted of S235J2 steel plates, 4mm and 10mm in thickness.

The test pieces with artificial imperfection were realized according to the sketches presented in figures 10. The holes and notches were filled with a Poxiline-type polymeric material, the surfaces being afterwards polished, sand blasted and cleansed with technical alcohol. Using the electric-arc thermal spraying procedure, a metallic layer was deposited on the surfaces with artificial flaws, using the following materials: Metco/ZnAW zinc wire, Ø1.62 mm and Metco/Tin Bronze wire, Ø1.62 mm.

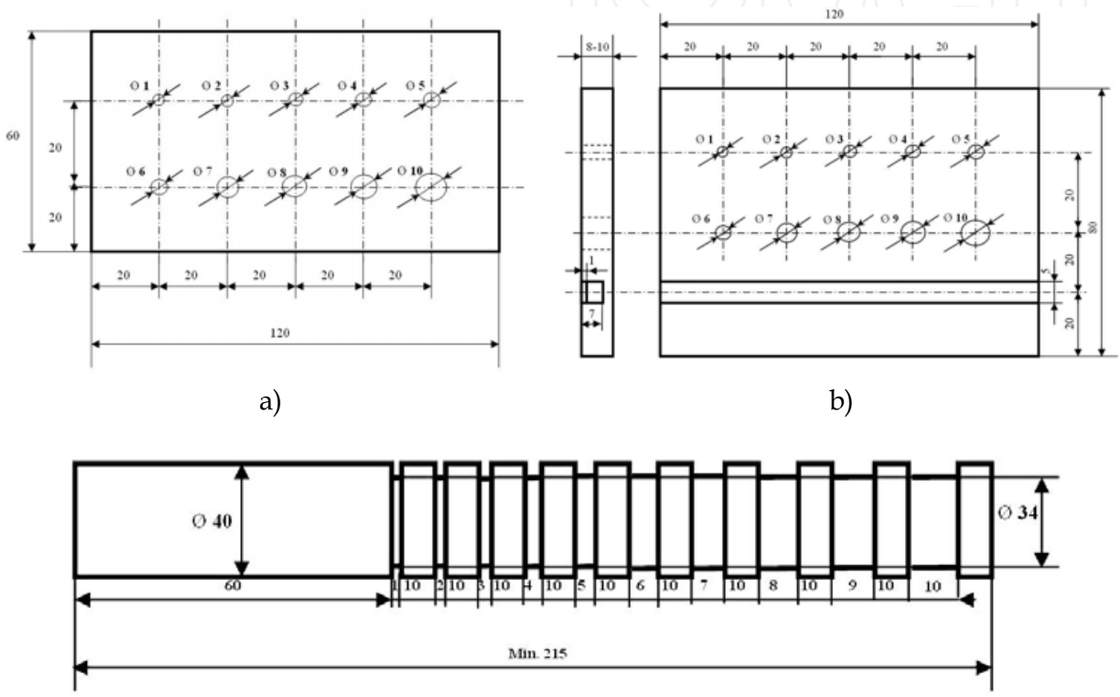

a) Type 1 test piece cu with Ø1 to Ø10 mm hole-type simulated defects
b) Type 2 test piece with Ø1 to Ø10 mm hole-type simulated defects and a notch (channel) with variable depth between 1 and 7 mm.
c) Type 3 test piece with 1 to 10 mm wide, simulated notches

Fig. 10. Test piece for thermographic test of the layers deposited by thermal spraying

Figure 11 presents, comparatively, the images of the test pieces with simulated flaws and their thermal images.

One could observe that the examination's sensitivity is influenced by the temperature of the examined part and by the coating material type. A lower temperature of the tested part leads to a more accentuated thermal contrast and a better flaw's detection. It was also established that a maximal thermal contrast is obtained after a certain period after the thermal activation (triggering the flashbulbs), and both the maximal temperature registered in the flaw area and the time after which the contrast is maximal depend on the flaw dimension.

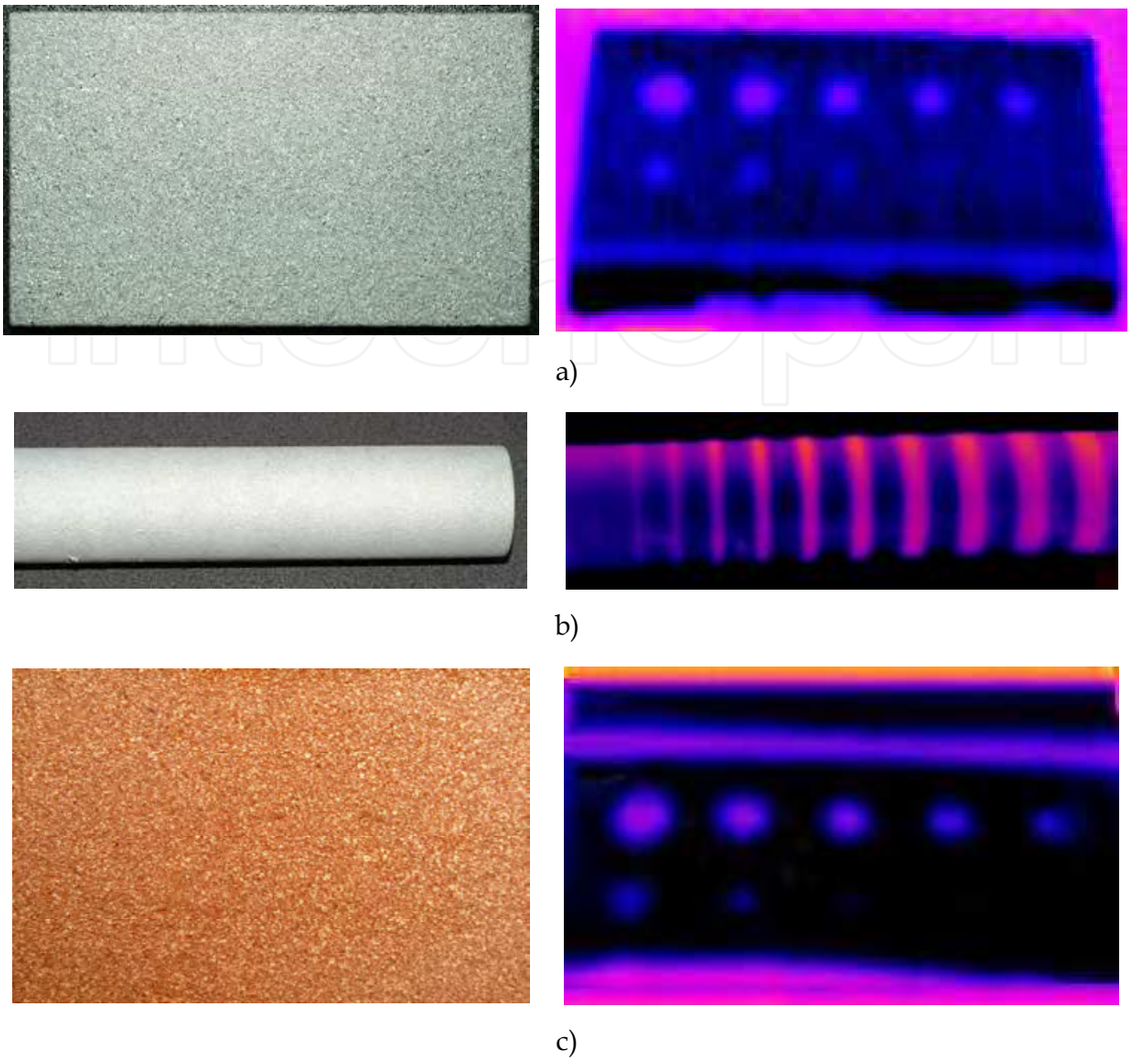

a) Test specimen - zinc coating,
b) Test specimen - zinc coating,
c) Test specimen - bronze coating

Fig. 11. Active thermography testing of metallic coatings;

The small flaws, close to the sensitivity limit of the active thermography method, could be identified by maximal contrast after a relatively short activation time following thermal activation and the large flaws can be best identified after a longer time interval following the activation period of the piece. The response time could be correlated with equivalent dimension of the imperfection.

Figure 12 presents the sensitivity curve for imperfections detection related to a thermal spraying coated surface obtained using electric-arc thermal spraying procedure, S235J2 steel for substrate and bronze wire (Metco/Tin Bronze cu Ø 1.62mm). Figure 13 presents the correlation between maximal surface temperatures recorded during the thermographic examinations versus the imperfections sizes, for the same type of coated surface.

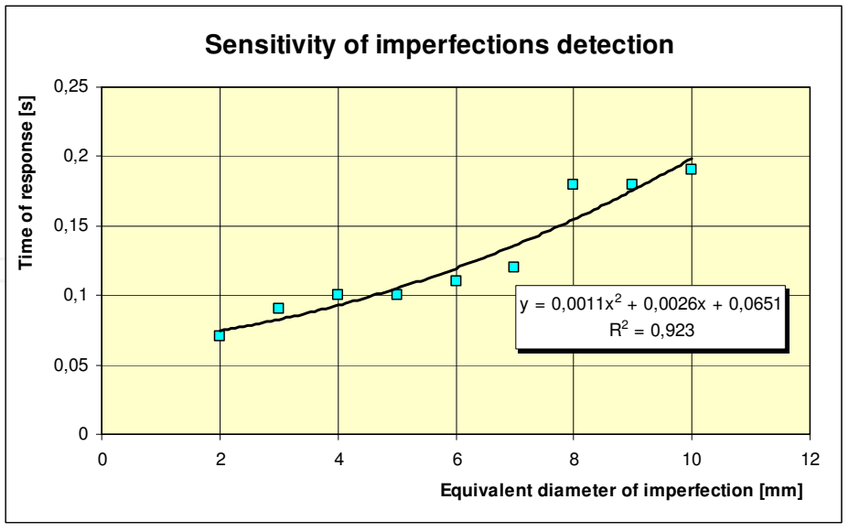

Fig. 12. Sensitivity of imperfections detection curve

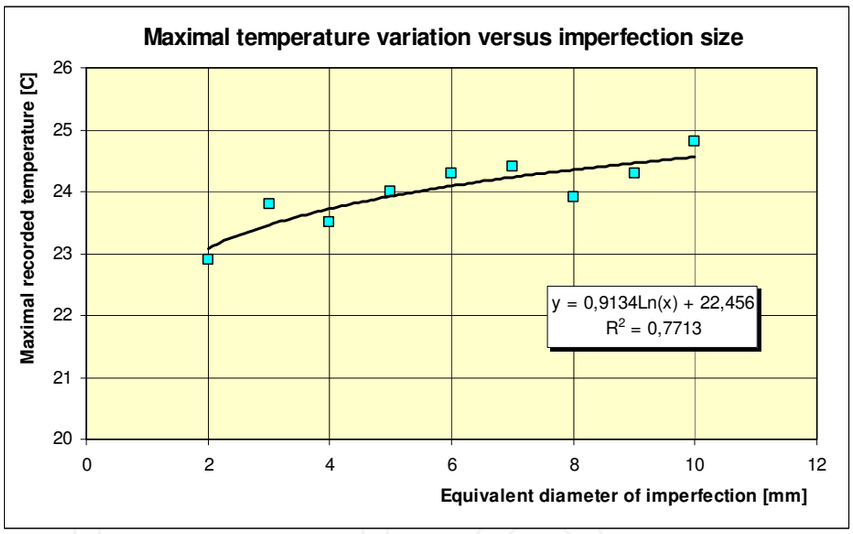

Fig. 13. Maximal temperature variation versus imperfection size

Experiments show that by using the active thermography method one can detect imperfection in coating layers deposited by thermal spraying. The notch-type flaws with the minimal width of 1 mm, respectively lack of adherence and porosity-type imperfection with equivalent diameters greater than 2 mm can be detected. Presented method is quantitative, and can be computerized by implementing of a complex informational system for intelligent data processing "artificial vision" type, based on the use of Hopfield and Kohonen neural networks (Bishop, 2006).

3.2 Studying a new laser-arc hybrid process dynamics

The use of IR thermography in welding process is mainly focused on developing process sensors with and without control (Huang et al., 2007; Mathieu et al., 2006), but also for

process comparison (Mattei et al., 2009), as a tool for validating the process models (Ilie et al., 2007) or, with a more complex approach, into integrated systems for evaluating the materials' weldability and controlling the welding process (Bîrdeanu A.-V. et. al, 2011b).

LASER-ARC hybrid welding process is not a new process (Steen & Eboo, 1979), and it is characterized, in the last decade, by an accelerated and continuous development towards industrial implementation (Staufer, 2005) and extending its applicability (Asai et al., 2009) with research focused on understanding and modelling the complex phenomena that characterizes the hybrid welding process (Cho et al., 2011; Zhu et al., 2004) and developing prediction models and tools to control it (Bidi et al., 2011).

Following this trend in laser-arch hybrid welding process development, with focus onto thin sheets joining applications a new laser-arc hybrid welding process was proposed (Bîrdeanu et al., 2009) which combines and couples the use of a pulsed laser source and a pulsed TIG process. The new laser – arc hybrid welding process was characterized, statistically modelled in order to evaluate the important process parameters and welding technologies were developed in order to compare its applicability as a replacement for other classical arc welding technologies (Bîrdeanu et al., 2011a) in respect to energy efficiency and process productivity.

The first steps in the development of the new laser-arc hybrid process required to investigate the hybrid process dynamics by doing bead-on-plate experimental work and using two video acquisition systems (one co-axial with the laser beam and one perpendicularly on the welding direction) in combination with thermal imaging of the processed area (figure 14) which proved that thermal imaging can be a tool fit for necessary investigations.

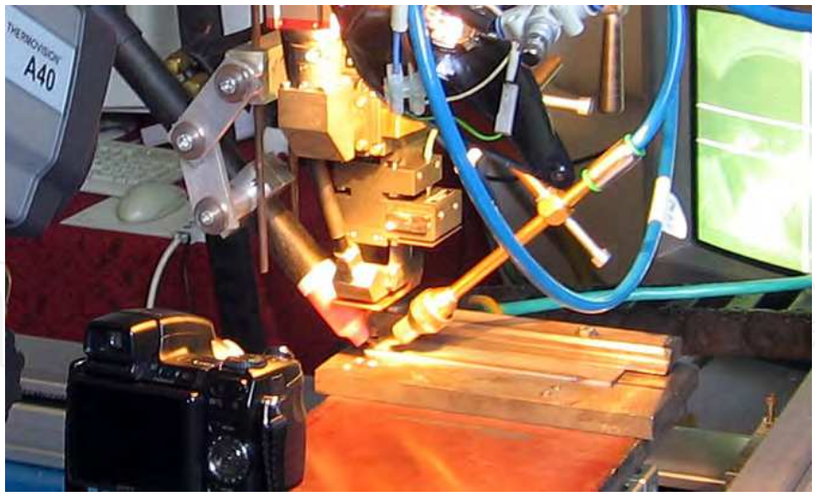

Fig. 14. Experimental system with 3 video acquisition systems: CCD camera, 25fps video camera, IR thermographical camera

While the video acquisition system allowed to reveal the way the two processes interact (figure 15), the IR thermography revealed important information regarding the intensity of the process interaction, the stability of the process by means of relative temperature variation of the processed area and why specific phenomena takes place (figures 16 and 17).

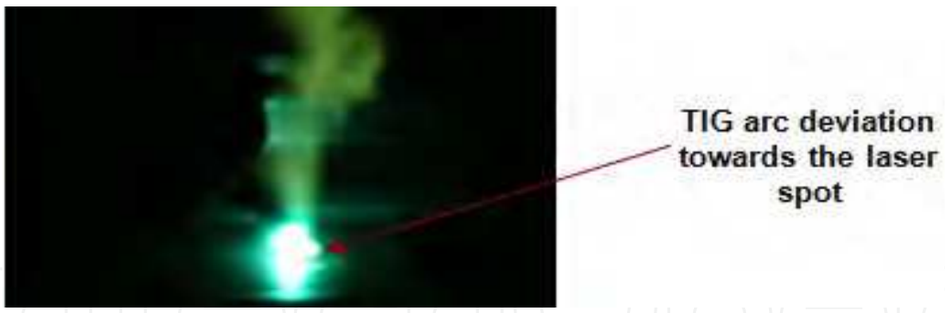

Fig. 15. LB (Laser Beam) generated plasma and TIG arc deviation toward the laser spot

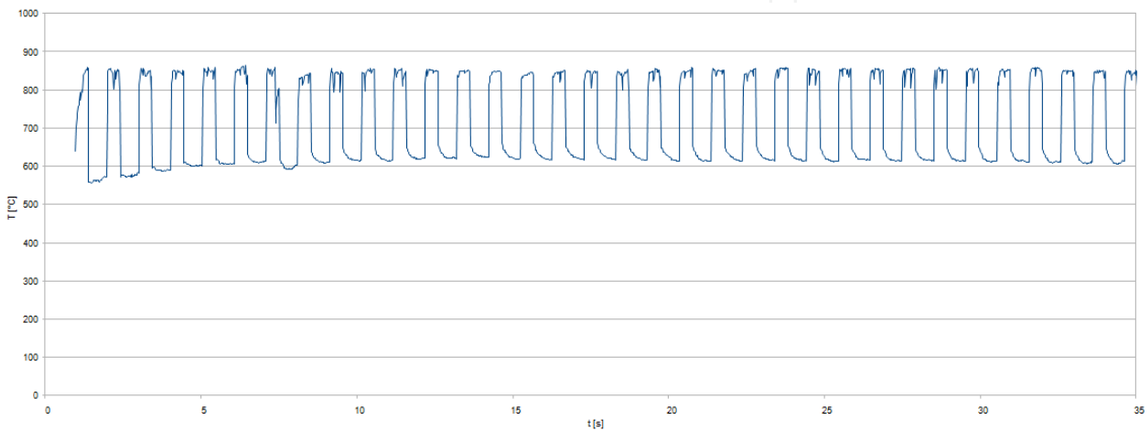

Fig. 16. Temperature variation of the monitored area (process variant: pulsed TIG-laser, Iav=28A, FrecvW=1Hz): Tmax=865.2°C; Tmin=591.807; Amplitude=273.4°C

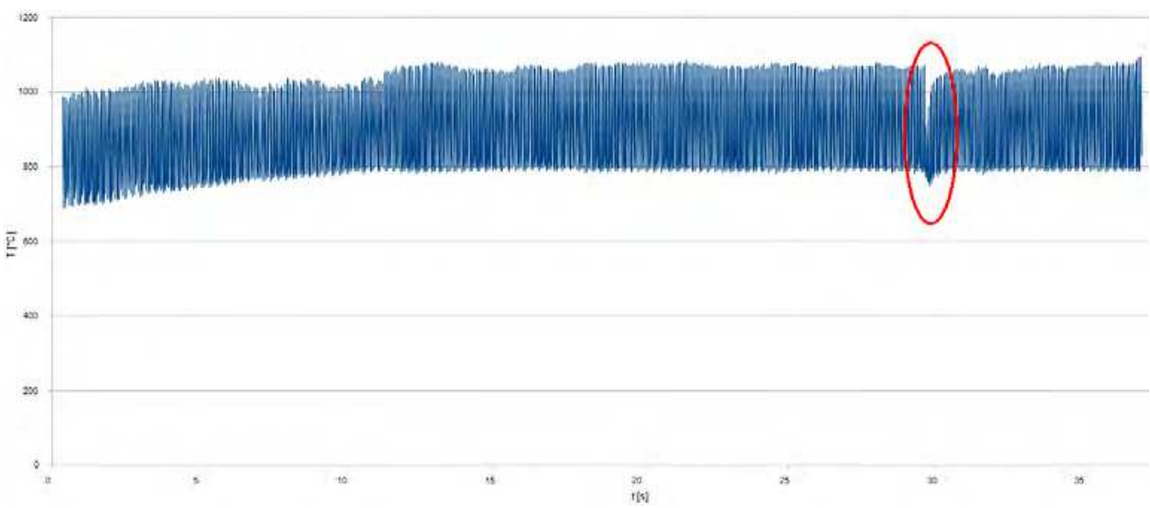

Fig. 17. Temperature variation of the monitored area for pulsed laser-TIG variant without laser protection gas at average TIG frequency (15Hz) – red circle indicates an instability

Though the temperature measurement was not calibrated, i.e. by determining a value for the emission coefficient of a point in the monitored area, the information provided by the thermal imaging acquisition system could be used to evaluate and characterize the process

due to the fact that the thermal imaging recordings were done by using the same experimental setup configuration and the relative values of the temperatures were compared by using the same processed area.

The three specific coupling situations (Bîrdeanu et al., 2009) for the pulsed laser-TIG hybrid welding process – during the peak current, during the base current and during the base-peak-base current transition – could be also be identified, beside using the normal video acquisition system, using the thermal imaging with peaks of increases in the temperature of the monitored area, especially for the low TIG current frequencies (figure 18).

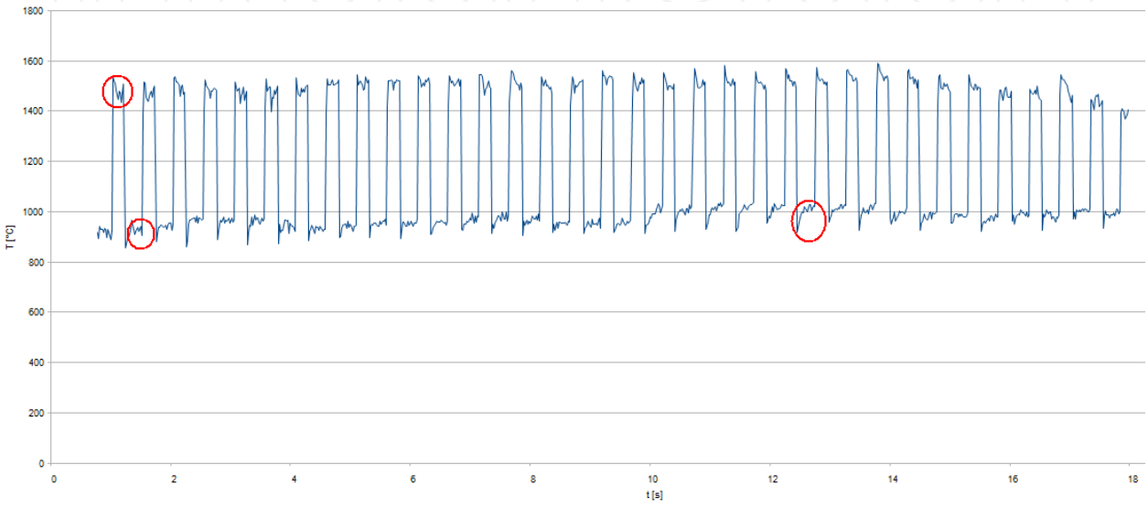

Fig. 18. Spikes in temperature variation (red circles) of the monitored area indicating the laser – arc interaction (process variant: pulsed TIG-LASER, TIG freq. 1Hz, ratTIG 40%)

The intensity of the process interactions (the hybrid coupling intensity) could be associated with the relative values of the temperature in the monitored area, i.e. higher average temperature of the monitored area were associated with an increase of the hybrid coupling and lower average temperatures were associated with lower hybrid coupling intensity. At the same time, sudden temperature changes of the monitored area could be associated with instabilities of the process (Fig. 17) while the overall temperature variation of the monitored area could be associated to the general degree of process stability.

Other important information regarding the process stability and the laser beam – electrical arc interaction was determined by evaluating the maximum temperature variation of the monitored area during the process and correlating that data with the video recordings of the two video acquisition systems. By processing the acquired data and evaluating the maximum temperature variation of the process, it was determined that the LASER-TIG variant (laser beam as leading process) was more stable and this could be observed both by using the visual video recording by observing the TIG arc stability due to its deviation towards the laser beam spot (Figure 19), by visual inspection of the weld (Figure 20), which could be correlated to a slight increase of the variation of the maximum temperature difference but at an increased absolute value of the temperature (Figure 21).

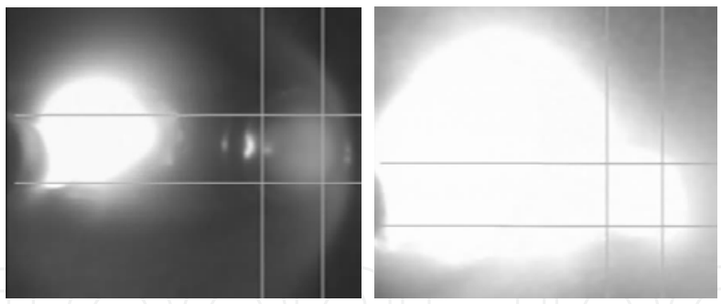

Fig. 19. Stronger influence on the pulsed TIG arc with pulsed laser beam as leading process both for base current and peak current regions (Iav=20A, TIG rat=40%, FTIG=1Hz) (Bîrdeanu et. al, 2009)

Fig. 20. Welded bead visual aspect for LASER-TIG variant

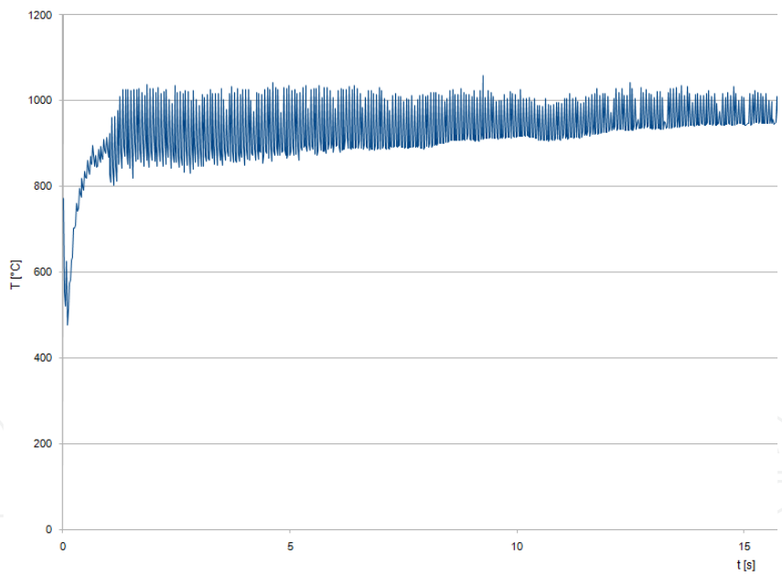

Fig. 21. Excerpt of temperature variation for LASER-TIG variant (Tmax: 1058.251^{o}C, Tmin: 861.738^{o}C, amplitude of temperature variation: 196.513^{o}C)

Beside the presented data, which was correlated to the other information acquired during the experimental work, it was also possible to correlate the temperature variation with other types of instabilities, e.g. spattering, which were afterwards verified by visual inspection of the weld and macroscopic analysis of transversal and longitudinal sections of the bead on plate in order to establish the direction for optimization of the process and develop welding technologies.

3.3 Using the IR thermography for monitoring and controlling of the Friction Stir Welding (FSW) process

3.3.1 General considerations

The worldwide achievements for FSW process monitoring are rather well known and important results were achieved in particular by using complex systems that ensure monitoring of the forces developed during the process and acting on the welding tools.

In this subchapter results of FSW research team from National R&D Institute for Welding and Material Testing – ISIM Timisoara are presented, regarding the possibilities of using infrared thermographic technique for monitoring the friction stir welding process (FSW).

Scientific results presented were obtained through complex FSW experimental programs, which included:

- FSW experiments on a wide range of materials (alloys of Al, Mg, Cu, Ti, steels, dissimilar materials) and optimization of the welding technologies;
- assisting the welding process using infrared thermography technique;
- interpretation of the temperature diagrams in correlation with the complex characterization of the welded joints (PT - Penetrant Tests, RT – Radiation Test, macro and microscopic analysis, static tensile and bending tests, hardness, surface roughness of welded joint, etc.).

The main researches objective was to demonstrate that the infrared thermographic technique can be used for monitoring the FSW process and to establish the limits for its application. The following research methods were used:

- simulation method of various defects type, i.e. holes, slots and implants, having different sizes
- real time tracing method in of the welding process - welded joints with different materials were made using optimized process parameters in previous research programs, the diagrams of temperature evolution were analyzed.
- samples were taken from welded joints, which were non-destructive and destructive analyzed and controlled, etc.
- comparing the results of the analysis diagrams of the evolution temperatures measured during the welding process, with the results obtained during the non-destructive and destructive control and evaluation of welded joints, for a wide range of types and thicknesses of metallic materials.

3.3.2 Experimental conditions

The experimental program was conducted on a specialized FSW machine (figure 22), with the following main technical characteristics:

- adjustable welding speed range: 60-480 mm/min.
- adjustable speed of the welding tool in range: 300-1450 rot/min.
- usable stroke (welding distance): 1000 mm.

Welding parts were butt positioned and rigidly fixed on a steel backing plate. The topping up of the machine with a monitoring and control system of the FSW process using infrared

Fig. 22. FSW machine from ISIM Timişoara, Romania

thermography can provide information on process stability, welding parameters stability, the appearance of some imperfections and/or defects, and also quality analysis of welds through the thermal image, as well as the adjustment and the optimization of the welding parameters through feedback connections.

The check-up of the operating principle in terms of identifying imperfections during the welding process, revealed that they can be evidenced through thermographic method because they represent a thermal barrier which are preventing the heat propagation inside of the object examined in accordance with its thermal characteristics, by having a different thermal conductivity of imperfections compared with the homogeneous material.

The temperature recording was realized on-line, using a Thermo – Vision A 40 M camera, at an acquisition rate of 25 images/s. The camera was placed on the welding equipment, (figure 22) in order to trace the intersection zone between the tool shoulder and the weld surface, on the back semi-circle zone (π/2), figure 23. The temperature recordings and processing were done by using the Therma Cam Researcher Pro specialised software.

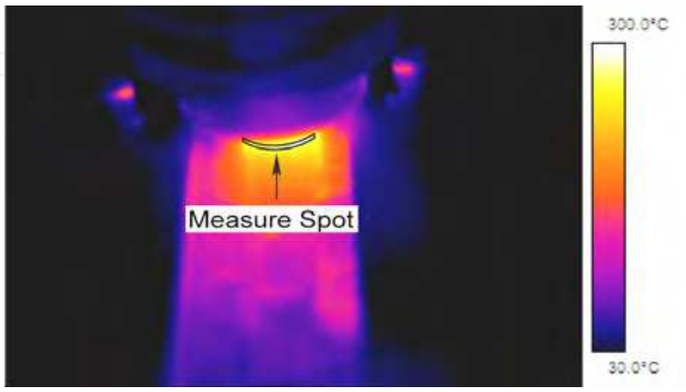

Fig. 23. Measure spot seen on the infrared image

Based on the recorded values from the temperature measurements, done with the infrared thermographic camera, the temperature evolution diagram during FSW welding process

could be obtained. The measurements were made on the joint line at a distance of 1 mm behind the welding tool shoulder (figure 24).

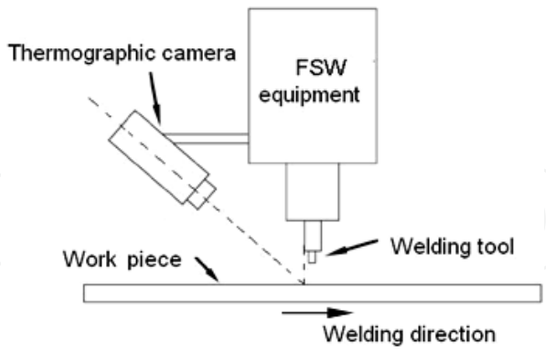

Fig. 24. Scheme of positioning for thermographic camera regarding to FSW machine

To determine how the temperature varies in material or in the materials (for the case of dissimilar materials) during welding, the measurements were made perpendicular to joint line at different distances from the weld start and the afferent variation graphs have been drawn.

3.3.3 Defects and simulation method

In order to verify the possibilities to apply the infrared thermography for on-line monitoring of the welded joints defects, an experimental program was developed, by using two types of artificially simulated defects, on EN AW 1050 sheet metal plates, having the dimensions 330x10 mm:

- inclusions , made perpendicularly on the plates and covered by FSW process, using a welding tool with the pin length bigger than the depth of the defects,
- defects made in the weld gap, on the frontal surface, in longitudinal direction of one of the plates which or butt welded by FSW process.

The experiments (Dehelean et al., 2008a) demonstrated the viability of infrared thermography in detection of the defects during the welding process. The experiments were based on using different forms and dimensions for the artificial defects made in the welded sheets. The sketch with the positions and the dimensions, for the case of artificially simulated defects having elliptical slits with variable width 2-6mm and constant depth h=4mm, are presented in figure 25.

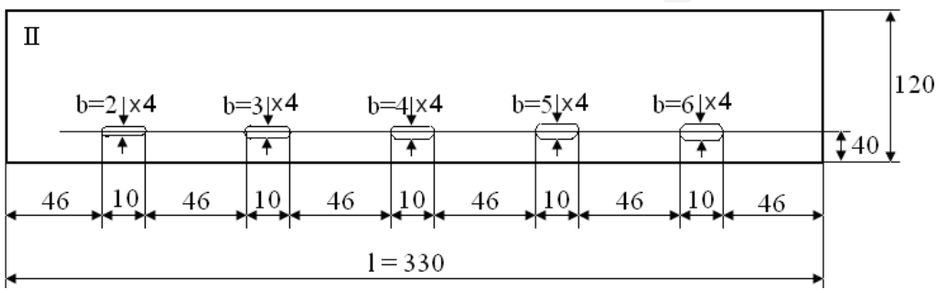

Fig. 25. Sketch of samples with simulated defects

In respect to the temperature evolution, recorded by the thermographic camera, for the welds done over the open slots, the recording T = f(l), presented in the oscillogram from figure 26 was obtained. Significant for the experiments are the "jumps" that appear on the temperature graphic, in front of the slits, due to local overheating.

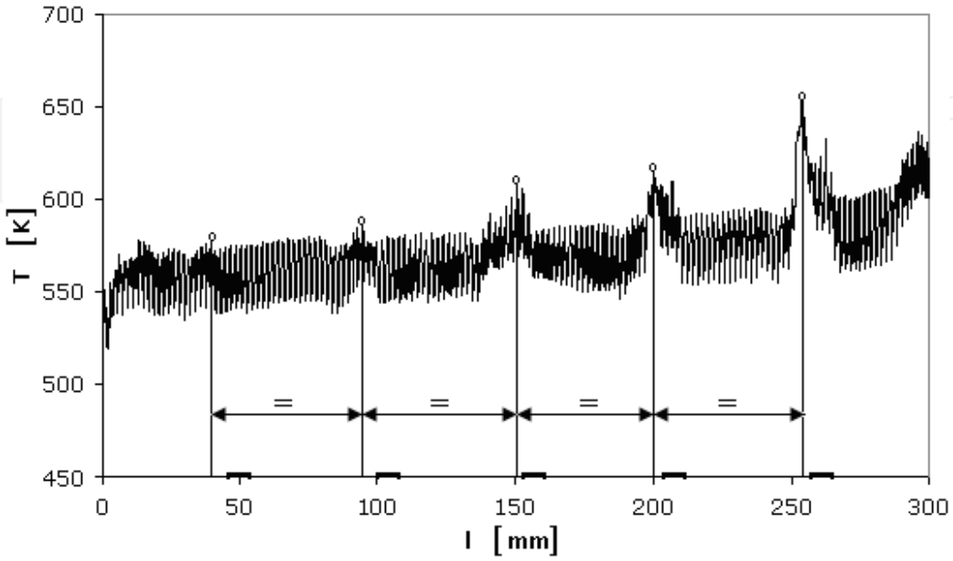

Fig. 26. MIT recording of the process

The performed researches reveal the real possibilities, both qualitative and quantitative, to detect the defects of FSW joints, using the infrared thermography method. Also, the good reproducibility of the results regarding localization of defects and dependence of the temperature variation with the dislocated volume by the defects, have been demonstrated.

The appearance of the peaks of temperature on the length of the welded joint and their systematic localizations in the defects zone, and in the working area of the welding tool respectively, was determined by the suddenly modification of the temperature gradient, caused by the thermal conductivity variation.

Also, it was concluded that, no matter the shape of the artificial defect, the minimum necessary volume to obtain a good evaluation of the thermographic recording can be determined (Safta, 2010).

3.3.4 Tracing method in real time of welding process for concrete applications

Based on the results obtained through the developed method by using simulated defects, one can mention good results in respect to the monitoring of the FSW process used for some concrete applications. By analyzing the temperature evolution diagram (figure 27), e.g. in case of welding of dissimilar alloys EN AW1200-EN AW 6082, uniformity is observed along the full length of the welded joint, after the welding process has been stabilized (after approximate 50-70 mm from the beginning of the welding process), (Cojocaru et al., 2011b) and, through X-ray analyse it was verified that the welded joint was free of defects. For such a welding application, after the stabilization process, the average temperature recorded in the joint line area was approximately 450˚C.

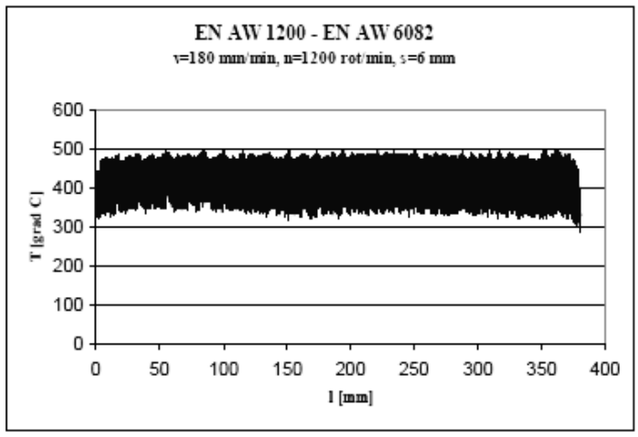

Fig. 27. Temperature evolution during FSW process

Comparing the temperature diagram evolution on a direction perpendicular to the joint line in the three moments of the realized measurements (figure 28) one can lay down several conclusions that may have an important role in the evaluation of welded joints and regarding the research results generally:

- before 50 mm of welding, the process is not yet stabilized and the optimum plasticizing temperature of materials (75-80% of melting temperature) was not reached.
- after the welding process stabilisation, the highest temperatures were recorded in the joint line area ≈ 465˚C.
- in interference zone of the welding tool shoulder and welding materials, to ±11mm from joint line, the following temperatures were recorded: 250-300˚C (EN AW 6082), respectively ~205-230˚C (EN AW 1200), (Cojocaru et al., 2011b).

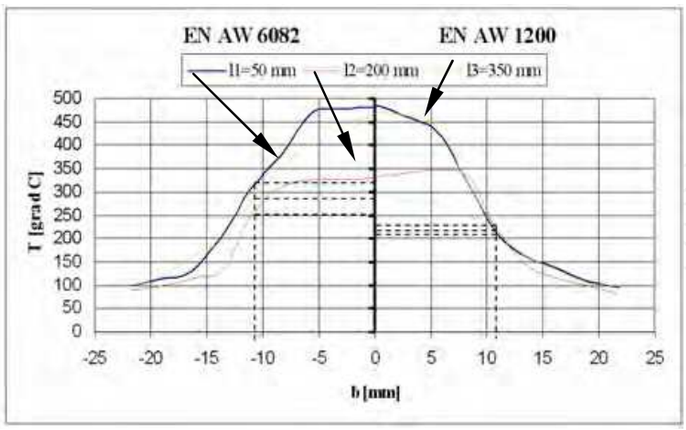

Fig. 28. Comparative evolution of temperatures

Another example is presented in figure 29 which shows the formation of a weld defect which occurred at friction stir welding of AZ31B magnesium alloy. The existence of the defect (revealed by X ray control) does determine a perturbation on the temperature diagram.

It was also observed an 80°C decrease of the temperature along the zone in which the defect occurred (lack of penetration), followed by an increase towards the stable values of the temperature after the defect position was overcome (Dehelean et al., 2008b). The cause of the defect was also identified being a malfunction/fault of FSW machine, which was characterized by ~ 40% reduction of rotational speed of welding tool While the welding speed was kept at the prescribed values. The temperature developed during the process is directly proportional with the rotational speed, it decreased with about 80°C, reaching values below the optimum temperature for plasticizing of the welded materials. As a result of the machine malfunction, there was an insufficient mixing of the materials, a consolidated nugget was not achieved and a tunnel type defect did appear (figure 29).

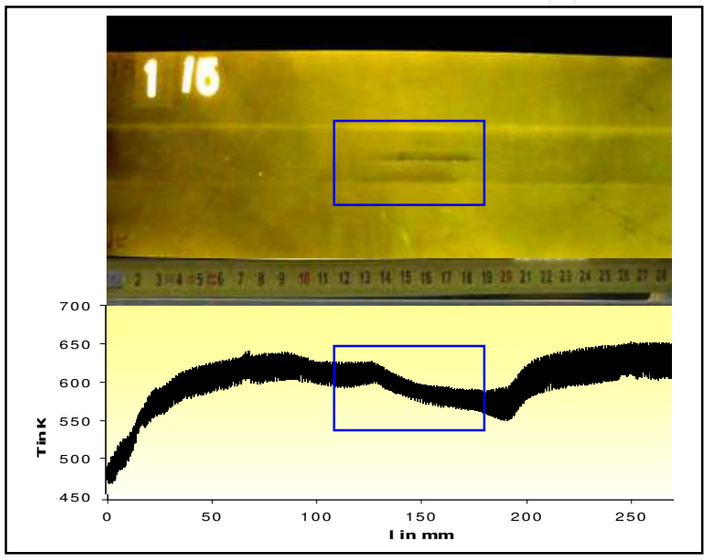

Fig. 29. Defect detection with radiographic control and correlation with temperature diagram

After remedying the machine's fault and returning to the initial set point of rotational speed, the welding process was carried out under optimal conditions, which could be revealed by the diagram of evolution of the temperature. This example also demonstrates the possibility to use infrared thermography for real time monitoring of the FSW process.

The same approach was used also for welding of steel, to obtain information about the temperature developed during the FSW process and for monitoring the process, by using infrared thermography. It was determined that for S235JR+N, S420MC and AISI 304L steels, after the 80-100mm from the beginning of the welding process, the temperature was constantly evolving around 980-1000°C (stable welding process), figure 30a. For friction stir welding of S235 steel, macroscopic aspect presented in figure 31a demonstrates the lack of defects and formation of nugget well consolidated in centre of the weld.

Another particular case where IR thermography allowed the identification of a faulty condition occurred during welding experiments of AISI 304L stainless steel. Analyzing the evolution of temperature diagram from figure 30 b one can notice that approximately 150mm from welding start there was a disturbance (area A). The subsequent verifications of welded sample revealed that in that area a 20% pin damage occurred (a volume of approx.

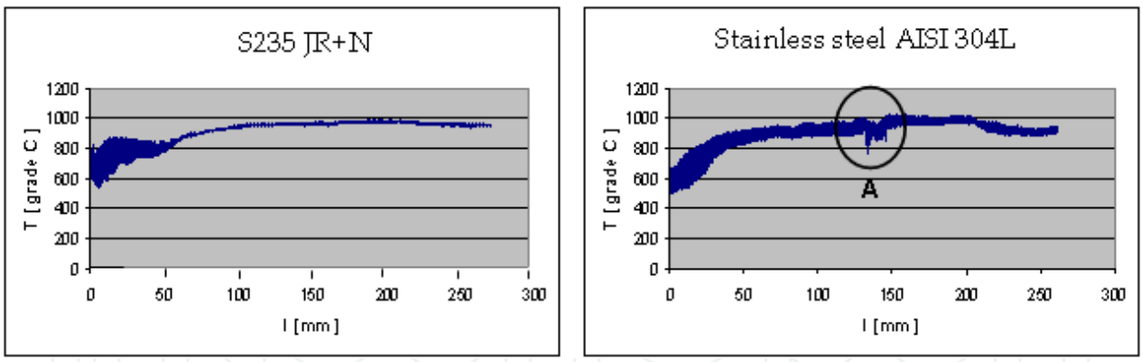

a) b)

Fig. 30. Evolution of temperature monitoring by thermographic camera

a) S 235 JR+N b) AISI 304L

Fig. 31. Macroscopic aspect of welded joints

20% of pin broke, which remained „implanted" in the welded material, figure 31b, the area marked B), (Cojocaru et al. 2011a).

This incident supports also the fact that the infrared thermography technique can be used for online monitoring of FSW welding process.

4. Conclusion

Worldwide, the infrared thermography usage is in continuous expansion and development both in material science and in engineering. Thermography method allows improving the characterization of new types of materials (composites, polymers), used more and more frequently in industrial products. As an example the polyethylene fracture behaviour in the presence of simulated imperfections was analyzed. It was found that recorded temperatures during the tensile tests are correlated with the local stress condition, induced by loading of the specimen with imperfections.

Using of thermography for process monitoring represents also actual trend in engineering. Beside its use as a monitoring or control tool, IR thermography proved to be also a good method to investigate and better understand the dynamics of a new laser-arc hybrid process and the acquired data could be correlated with the information and observations gathered using the usual video recording system and the specific analysis of the welding process results. It was also demonstrated that the system used for on-line monitoring of the FSW process has a good reproducibility for a large range of defects with different sizes and positions.

5. Acknowledgment

This work was partially supported by the Romanian National Authority for Scientific Research, project PN-09-160203, project PN 09-160101, PN-09-160 104 (2009-2010) and partially supported by the National Research Plan PNCDI 2: Frame 4: "Partnerships in priority areas", project 72174, acronym TIMEF, financed by the UEFISCDI (2008-2011).

6. References

Asai, S.; Ogawa, T.; Ishizaki, Y.; Minemura, T.; Minami, H. & Miyazaki, S. (2009). *Application of Plasma-MIG Hybrid Welding to Dissimilar Joint between Copper and Steel*, International Institute of Welding Doc. No. XII-1972-09

Avdelidis, N.P.; Ibarra-Castanedo, C.; Theodorakeas, P.; Bendada, A.; Saarimaki, E.; Kauppinen, T.; Koui, M. & Maldague, X. (2010). NDT characterisation of carbon-fibre and glass-fibre composites using non-invasive imaging techniques, *10th International Conference on Quantitative Infrared Thermography*, July 27-30, 2010, Qubec, Canada

Balageas, D.L.; Levesque,P.; Brunet,P.; Cluzel, C.; Déom A. & Blanchard, L. (2006). Thermography as a routine diagnostic for mechanical testing of composites, In: *Quantitative Infrared Thermography –The 8th QIRT,* Padova, Italy, June 27-30, 2006

Bidi, L.; Mattei, S.; Cicala, E.; Andrzejewski, H.; Le Masson, P. & Schroeder, J. (2011). *The use of exploratory experimental designs combined with thermal numerical modelling to obtain a predictive tool for hybrid laser/MIG welding and coating processes*, Optics & Laser Technology 43, pp. 537-545, ISSN 0030-3992

Bishop, C.M. (2006). *Pattern recognition and machine learning*, Springer, 2006, ISBN 978-0-387-31073-2, http://www.springer.com/978-0-387-31073-2

Bîrdeanu, A.-V.; Ciucă, C. & Iacob, M. (2011a). Pulsed LASER-TIG hybrid welding of coated unalloyed steel thin sheets, *Proceedings of The 5th International Conference Innovative technologies for joining advanced materials*, ISSN 1844-4938, Timişoara, Romania, June 16-17, 2011

Bîrdeanu, A.–V.; Ilie, M; Stoica, V. & Verbitchi, V. (2011b). Integrated experimental system for evaluating polymers laser weldability, real-time monitoring and control, *Proceedings of Modern Technologies, Quality and Innovation-ModTech International Conference*, ModTech Publishing House Chisinau, Republic of Moldova, 25 – 27 May, ISSN 2069-6736

Bîrdeanu, V.; Dehelean, D. & Savu, S. (2009). *Laser - TIG hybrid micro-welding process developments*, BID - ISIM Welding & Material Testing, No. 4 (December 2009), pp. 37-42, ISSN 1453-0392

Boțilă, L.; Murariu, A. C.; Cazacu, A. & Ciucă, C. (2011). Applications of infrared thermography in nondestructive examination of materials and welding, *Revista Sudura*, no. 1/2011, pp. 6-13, ISSN 1453-0384

Bremond, P. (2010). Full Field Experimental stress/strain analysis by Thermographic stress analyser for fatigue crack detection during HCF Testing. Examples in Automotive and Aircraft industry, *10th International Conference on Quantitative Infrared Thermography*, July 27-30, 2010, Qubec, Canada

Cho, Y.T.; Cho, W.I. & Na, S.J. (2011). *Numerical analysis of hybrid plasma generated by Nd:YAG laser and gas tungsten arc*, Optics & Laser Technology 43, pp. 711-720, ISSN 0030-3992

Choi, M.Y.; Park, J.H.; Kim, W.T.; Lee, S.S.; Kim, K.S.; Kang, K.S. (2008). Predicting the Dynamic Stress Concentration Factor Using the Stress Measuring Method Based on the Infrared Thermography, *9th International Conference on Quantitative Infrared Thermography*, July 2-5, 2008, Krakow, Poland

Cojocaru, R.; Boțilă L.; Ciucă, C. (2011a) Possibilities to apply the friction stir welding (FSW) to steels, *Revista Sudura,*No.1 (March 2011), pp.34-40, ISSN 1453-0384

Cojocaru, R.; Boțilă L.; Ciucă, C. (2011b) Friction stir welding of EN EW 1200-EN AW6082 aluminum alloys, *Proceedings of the 15th International Conference Modern Technologies, Quality and Innovation MODTECH New Face of T..M.C.R.,* Vol. I, pp.277-280, ISSN 2069-6736, Vadul lui Vodă, Chişinău, Republic of Moldova, 25-27 May, 2011

Dehelean, D.; Safta, V.; Cojocaru, R.; Hälker, T.; Ciucă, C. (2008a) Monitoring the quality of friction stir welded joints by infrared thermography, *International Conference Safety and Reliability of Welded Components in Energy and Processing Industry,* Graz, Austria, 2008

Dehelean, D.; Cojocaru, R.; Boțilă, L.; Radu, B. (2008b) Friction stir welding of aluminum-magnesium dissimilar joints, *International Conference Welding,* Subotica, Serbia, 2008

Galietti, U. & Palumbo, D., (2010). Application of thermal methods for characterization of steel welded joints, *10th International Conference on Quantitative Infrared Thermography*, July 27-30, 2010, Qubec, Canada

Grellmann, W.; Bierögel, C.; Langer, B. (2003). Modern mechanical methods of technical polymer diagnostics *In: Proceeding of Amsler Symposiums: World of Dynamic Testing*, pp. 117-126, Gottmardingen, Germany, 19-22 May, 2003

Grellmann, W. & Seidler, S. (2001). Deformation and Fracture Behaviour of Polymers, *Series: Engineering Materials*, ISBN: 978-3-540-41247-2, Springer-Verlag, New York

Huang, R.-S.; Liu L.-M. & Song G. (2007). *Infrared temperature measurement and interference analysis of magnesium alloys in hybrid laser-TIG welding process*, Materials Science and Engineering: A, Volume 447, Issues 1-2, 25 February 2007, pp. 239-243, ISSN 0921-5093

Huebner, S.; Stackelberg, B.V. & Fuchs, T (2010) Multimodal Defect Quantification, *10th International Conference on Quantitative Infrared Thermography*, July 27-30, 2010, Qubec, Canada

Ilie, M.; Kneip, J.-C.; Mattei, S.; Nichici, A.; Roze, C. & Girasole T. (2007). *Through-transmission laser welding of polymers - temperature field modeling and infrared investigation*, Infrared Physics & Technology, Volume 51, Issue 1, July 2007, pp. 73-79, ISSN 1350-4495

Kruczek, T. (2008). Particular applications of infrared thermography temperature measurements for diagnostics of overhead heat pipelines, *9th International Conference on Quantitative Infrared Thermography*, July 2-5, 2008, Krakow, Poland

Mathieu, A.; Mattei, S.; Deschamps, A.; Martin, B. & Grevey D. (2006). *Temperature control in laser brazing of a steel/aluminium assembly using thermographic measurements*, NDT & E International, Volume 39, Issue 4, June, pp. 272-276, ISSN 0963-8695

Mattei, S.; Grevey, D.; Mathieu, A. & Kirschner, L. (2009). *Using infrared thermography in order to compare laser and hybrid (laser+MIG) welding processes*, Optics & Laser Technology, Volume 41, Issue 6, September 2009, pp. 665-670, ISSN 0030-3992

Murariu, A. C. & Crâsteți, S. (2011). Nondestructive testing options by active thermography of thermal spraying coated surfaces, *Revista Sudura*, no. 1/2011, pp. 14-18, ISSN 1453-0384

Murariu, A. C.; Safta, V. I. & Mateiu, H. S. (2010). Long-term behaviour of polyethylene PE 80 pressurized pipes, in presence of longitudinal simulated imperfections, *Revista Materiale Plastice*, Vol. 47, No.3, pp. 263-266, ISSN: 0025-5289

Murariu, A.C.; Safta, V.I. & Fleşer, T. (2008). Investigations regarding the thermoplastic resistance evaluation with simulated imperfections, *Strength of Materials Laboratory at 85 years International Conference*, University POLITEHNICA of Timisoara Faculty of Mechanical Engineering Department of Strength of Materials, 2008, In: Key Engineering Materials Vol. 399, pp. 131-138, Trans Tech Publications, Switzerland, 2009, ISSN 1013-9826

Murariu, A.C. & Bîrdeanu, V. (2007). Experimental Method (LSI) for Planar Simulated Imperfections for Remaining Life Assessment of the Thermoplastic Pipe Networks, In: *The International Conference on Structural Analysis of Advanced Materials - ICSAM 2007*, Patras, Grece, 2-6 sept., 2007

Murariu, A.C. (2007). TT-IRT Hybrid Testing Method Applied in the Study of PE 80 Polyethylene Behaviour in the Presence of Simulated Imperfection, *The 5th International conference Structural integrity of Welded Structures*, 20-21 Nov., Timişoara, Romania, 2007

Pieczyska, E.A.; Nowacki, W.K.; Tobushi, H. & Hayashi, S. (2008). Thermomechanical properties of shape memory polymer SMP subjected to tension and simple shear process , *9th International Conference on Quantitative Infrared Thermography*, July 2-5, 2008, Krakow, Poland

Safta, V. (2010) Application of infrared thermopgraphy in the non-destructive examination of friction stir welds, *Welding &Material Testing BID ISIM,* No1/2010, pp.29-40, ISSN 1453-0392

Sahli, S; Fissette, S. & Maldague, X. (2010). Infrared Image Processing for Online Quality Control in Laser Welding, *10th International Conference on Quantitative Infrared Thermography*, July 27-30, 2010, Qubec, Canada

Staufer, H. (2005) Laser hybrid welding and laser brazing: state of the art in technology and practice by the examples of the AudiA8 and VW Phaeton, in: *Proceedings of the third International WLT Conference on Lasers in Manufacturing*

Steen, W.M. & Eboo, M. (1979). *Arc Augmented Laser Welding*. Met. Constr. 11, H. 7, pp. 332-333, 335

Rajic, N. (2004). Modelling of thermal line scanning for the rapid inspection of delamination in composites and cracking in metals, *DSTO Publications Online,* Available from http://hdl.handle.net/1947/4097

Thiemann, C.; Zaeh, M.F.; Srajbr, C. and Boehm, S. (2010). Automated defect detection in large-scale bonded parts by active thermography, *10th International Conference on Quantitative Infrared Thermography*, July 27-30, 2010, Qubec, Canada

Yang, B.; Liaw, P.K.; Wang, H.; Huang, J.Y.; Kuo, R.C. & Huang, J.G. (2003). Thermography: A New Nondestructive Evaluation Method in Fatigue Damage, In: *TMS Online JOM-e*: *A Web-Only Supplement to JOM*, Available from http://www.tms.org/pubs/journals/jom/0301/yang/yang-0301.html

Wang, H.; L. Jiang,L; He, Y. H.; Chen L. J. & P. K. Liaw, P. K. (2002). Infrared imaging during low-cycle fatigue of HR-120 alloy, Metallurgical and Materials Transactions A, Vol.33 pp. 1287–1292 DOI: 10.1007/s11661-002-0231-1

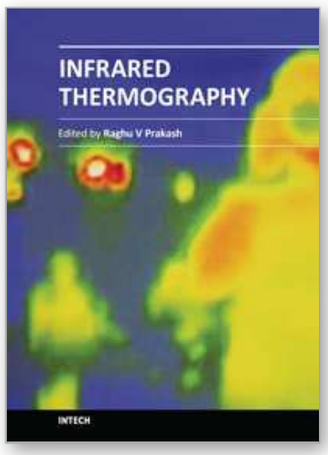

Infrared Thermography

Edited by Dr. Raghu V Prakash

ISBN 978-953-51-0242-7
Hard cover, 236 pages
Publisher InTech
Published online 14, March, 2012
Published in print edition March, 2012

Infrared Thermography (IRT) is commonly as a NDE tool to identify damages and provide remedial action. The fields of application are vast, such as, materials science, life sciences and applied engineering. This book offers a collection of ten chapters with three major sections - relating to application of infrared thermography to study problems in materials science, agriculture, veterinary and sports fields as well as in engineering applications. Both mathematical modeling and experimental aspects of IRT are evenly discussed in this book. It is our sincere hope that the book meets the requirements of researchers in the domain and inspires more researchers to study IRT.

How to reference

In order to correctly reference this scholarly work, feel free to copy and paste the following:

Alin Constantin Murariu, Aurel - Valentin Bîrdeanu, Radu Cojocaru, Voicu Ionel Safta, Dorin Dehelean, Lia Boţilă and Cristian Ciucă (2012). Application of Thermography in Materials Science and Engineering, Infrared Thermography, Dr. Raghu V Prakash (Ed.), ISBN: 978-953-51-0242-7, InTech, Available from: http://www.intechopen.com/books/infrared-thermography/applications-of-thermography-in-materials-science-and-engineering

INTECH
open science | open minds

InTech Europe
University Campus STeP Ri
Slavka Krautzeka 83/A
51000 Rijeka, Croatia
Phone: +385 (51) 770 447
Fax: +385 (51) 686 166
www.intechopen.com

InTech China
Unit 405, Office Block, Hotel Equatorial Shanghai
No.65, Yan An Road (West), Shanghai, 200040, China
中国上海市延安西路65号上海国际贵都大饭店办公楼405单元
Phone: +86-21-62489820
Fax: +86-21-62489821

IntechOpen